# Cocrystal Engineering of Itraconazole with Suberic acid via Rotary Evaporation and Spray Drying

Jingwen Weng[1,#], Si Nga Wong[1,#], Xiaoyan Xu[1], Bianfei Xuan[1], Chenguang Wang[2], Ruipeng Chen[3], Changquan Calvin Sun[2], Richard Lakerveld[3], Philip Chi Lip Kwok[4], Shing Fung Chow[1,*]

[1]Department of Pharmacology and Pharmacy, Li Ka Shing Faculty of Medicine, The University of Hong Kong, Pokfulam, Hong Kong

[2]Pharmaceutical Materials Science and Engineering Laboratory, Department of Pharmaceutics, College of Pharmacy, University of Minnesota, USA

[3]Department of Chemical and Biologic Engineering, The Hong Kong University of Science & Technology, Clear Water Bay, Kowloon, Hong Kong

[4]School of Pharmacy, The University of Sydney, New South Wales, Australia.

# *Equal contribution*

* *Corresponding author*

Shing Fung Chow
Department of Pharmacology and
Pharmacy
Li Ka Shing Faculty of Medicine
The University of Hong Kong
L2-08B, Laboratory Block,
21 Sassoon Road, Pokfulam, Hong
Kong
Email: asfchow@hku.hk
Tel: +852-39179026
Fax: +852-28170859

## ABSTRACT

Cocrystallization represents an emerging approach to tackle the issues associated with pharmaceutical product performance and processing, owing to its capability of modifying a variety of physicochemical properties. In this study, we sought to modify the crystal form of itraconazole (ITZ) with suberic acid (SUB) via rapid solvent removal methods, namely rotary evaporation and spray drying. A phase pure ITZ-SUB cocrystal, which could not be obtained by traditional cocrystallization methods, was successfully prepared by rotary evaporation. The new cocrystal was confirmed by powder X-ray diffraction, differential scanning calorimetry, and Fourier-transform infrared spectroscopy. Spray drying was further employed for particle engineering of ITZ-SUB to achieve optimal pulmonary delivery. By manipulating the critical processing parameters, inhalable ITZ-SUB agglomerates with mass median aerodynamic diameter of 2.56 ± 2.27 μm and fine particle fraction of 64.10% w/w were reproducibly prepared. The inhalable powders contained mainly co-amorphous ITZ-SUB, while a small portion of cocrystals still exists. Compared with the raw ITZ, the intrinsic dissolution rate of ITZ-SUB cocrystal was ~39 times faster, and a significantly larger fraction of ITZ-SUB agglomerates were dissolved after 180 min of the test. Besides, both products remained stable after 1-month storage at 60 °C.



**Keywords:** Itraconazole, Cocrystal, Cocrystal agglomerate, Spray drying, Dry powder inhaler formulation, Aerosol performance, Dissolution

## 1. Introduction

Recent advances in cocrystal engineering have ignited mounting interests in the development of next-generation formulations for improved drug delivery. Its promise in tuning the physicochemical properties of problematic drugs, including solubility, dissolution performance, hygroscopicity, and compressibility has been proven and well-documented, thus offering vast opportunities for tailored therapy according to the clinical needs of individual patients.[1, 2] Other merits pertaining to cocrystallization involve its high-level applicability for a wide array of APIs, both weakly ionizable and neutral compounds, which have either limited or no capacity for salt formation.[3, 4]

The successful pharmaceutical cocrystal fabrication lies in both prudent selection of crystal formers and effective synthetic approaches. Kinetically driven processes, namely rapid solvent removal via rotary evaporation and spray drying, have been shown to be effective for the preparation of elusive cocrystals, which could not be obtained by conventional methods, such as solid state grinding, slurring, and slow evaporation.[5, 6] Despite the efficiency and ease-of-use of rotary evaporation in initial cocrystal screening stage, its application in mass production is severely hindered since it is a batch process with limited scalability. In contrast, spray drying which produces dry powder through rapid drying of a liquid or slurry in an environment of hot air[7], is a well-established processing technology for particle engineering and industrial scale-up. Large batches of cocrystal formulations with consistent quality can be continuously manufactured with high production efficiency.[7] Notably, it also allows the optimization of pharmaceutical properties and aerosolization attributes (e.g., size, density, and morphology), particularly for pulmonary drug administration, through modifying critical processing parameters, such as feed solid concentration and gas atomization flow rate.[8-10] Although spray drying holds the promise for efficient development of inhalable cocrystal formulations, there are only a few existing studies which probed into such emerging application.

Both the choice of formulation compositions and the design of particles with good dispersibility are critical to ensure adequate lung deposition. The particle aerodynamic diameter ($d_A$) is one of the most important parameters that impacts particle deposition into the lung.[13] It is defined as the diameter of a unit-density spherical particle, which gives the

same settling velocity as the non-spherical particle of interest, and as expressed in eqn. (1):

$$d_A = d_V\sqrt{\frac{\rho}{\chi\rho_0}} \qquad \text{Eqn. (1)}$$

where $d_V$ is the equivalent volume diameter of the particle of interest, $\rho$ is the particle density, $\rho_0$ is the reference density (1 g·cm$^{-3}$), and $\chi$ is the dynamic shape factor. In general, aerosols with $d_A$ ranging from 1 to 5 $\mu$m are suitable for pulmonary deposition.[14] Particles with $d_A$ > 5 $\mu$m mostly deposit in the upper respiratory tract by inertial impaction, while particles with $d_A$ < 1 $\mu$m tend to remain air-bone in the airways and are eventually exhaled out during the normal breathing cycle. Nevertheless, particles with $d_A$ ranging 1-3 $\mu$m penetrate into the deep lung region better, thus they are recognized as the most optimal fraction for delivery to the alveoli.[15]

Itraconazole (ITZ, Figure 1) is a synthetic triazole antifungal drug commercially available in its amorphous form, Sporanox®.[16] The use of oral ITZ has been approved by U.S. FDA since 1992 and is indicated for blastomycosis, histoplasmosis, aspergillosis and onychomycosis.[16] Of particular merit, it is strongly recommended by the Infectious Diseases Society of America (IDSA) for the prophylaxis of invasive pulmonary aspergillosis (IPA), a severe pulmonary infection of the *Aspergillus species* with high morbidity and mortality rates (30-90%).[17, 18] Through drug repositioning, it is also found to be effective against several types of carcinoma, especially non-small-cell lung cancer.[19-21] Nonetheless, as a Class II drug in the Biopharmaceutics Classification System (BCS) that is practically insoluble in water, ITZ requires high oral dose (normally 200 mg daily) to achieve adequate and sustained concentration in the lungs, causing unintended systemic toxicities. Besides, the pharmacokinetic variability of ITZ may hamper its therapeutic efficacy.[22] Recent studies for improving the therapeutic outcomes of ITZ includes separate efforts for developing inhalable ITZ powder formulations for targeted pulmonary delivery,[23-25] and for ameliorating its solubility through various crystal engineering approaches, such as salt formation and cocrystallization.[26-28]

In the context of crystal engineering, Shevchenko et al. reported that cocrystals of ITZ with C2−C7 aliphatic dicarboxylic acids were obtained from a combination of slow evaporation using a 1:1 mixture of tetrahydrofuran with chloroform and solvent-assisted

milling using acetone. However, they did not evaluate the solubility and dissolution performance of the resulting cocrystals. Interestingly, attempts of preparing ITZ cocrystals with suberic acid, azelaic acid and sebacic acid (C8-C10) had failed via the same method, despite their structural resemblance with other shorter-chain acids.[27] It is not uncommon that cocrystallization with longer-chain acids usually fails or exhibits low efficiency via conventional methods, where the carbon number 8 appeared to be the threshold of successful cocrystallization.[29, 30] We herein conjecture that such phenomenon may be ascribed to the thermodynamic instability or the relatively high activation energy for cocrystal formations. Both can be overcome by kinetic entrapment through fast crystallization from a solution. Thus, the goals of this work were to: (1) prepare and characterize a fast dissolving ITZ cocrystal with long-chain acid, i.e., suberic acid (SUB), which could not be prepared previously by solvent assisted milling method, by rapid solvent removal; and (2) investigate the potential of integrated crystal and particle engineering through one-step spray drying process for continuous fabrication of a dry powder inhalation (DPI) formulation of ITZ-SUB cocrystal. Different spray drying attributes, including feed solid concentrations and gas atomization flow rates, were used to prepare the ITZ-SUB powders with desired aerosolization performance for pulmonary delivery.

## 2. Experimental Section

### 2.1. Materials

Itraconazole (ITZ) (purity ≥ 98.5%) was supplied from Yick Vic Chemicals & Pharmaceuticals Ltd (Hong Kong, China). Suberic acid (SUB) was purchased from Alfa Aesar (Ward Hill, MA, USA. Chloroform (CFM), ethanol (EtOH), tetrahydrofuran (THF) and acetonitrile (ACN) of analytical grade were obtained from Merck KGaA (Darmstadt, Germany). Water was purified through a Direct-Q water purifier (Water Corp., Milford, MA). Ammonium acetate was purchased from Sigma Aldrich (St Louis, Mo, USA) and analytical grade acetic acid was obtained from BDH Laboratory Supplies (Dorset, England). Hydrochloric acid 37% was provided by RCI Labscan Ltd (Bangkok, Thailand).

### 2.2. Preparation of Cocrystals by Rotary Evaporation

Equimolar amounts (0.425 mmol) of ITZ (100 mg) and SUB (24.69 mg) were dissolved in a 100 mL mixture of EtOH and CFM (4:1 v/v). Subsequently, the organic solvent was removed using a rotary evaporator (Büchi, Germany) under a vacuum (90 mm Hg) achieved by a vacuum pump (Millipore, USA) with the rotary flask rotating at a speed of 40 rpm while being immersed in a water bath at 60 °C, resulting in an evaporation speed of around 6.9mL/min. The resulting product was dried in an oven at 80 °C overnight to remove residual solvent and gently grounded to a fine powder for further analysis. All samples were stored in parafilm-wrapped plastic vials after drying in a double-zipped bag to avoid significant moisture sorption.

### 2.3. Determination of the Solubility of ITZ and SUB in Organic Solvents

Excess amounts of ITZ and SUB were separately added in screw-capped test tubes with 5 mL of different organic solvents and shaken for 72 hours. To make the supersaturated suspension of ITZ and SUB in the mixture of EtOH and CFM (4:1 v/v), an excess amount of ITZ was dissolved in 1 mL CFM initially, followed by the addition of 2 mL EtOH. Subsequently, an excess amount of SUB was poured in. Finally, another 2 mL EtOH was added. Samples were withdrawn and filtered through 0.45 μm nylon syringe filters (Membrane Solutions, Hong Kong), followed by dilution to appropriate concentrations for HPLC assay (see Section 2.3).

### 2.4. High Performance Liquid Chromatography (HPLC)

The concentrations of ITZ and SUB in the solubility study were determined using an HPLC equipped with a diode array detector (Agilent 1200 series, Agilent Technologies, USA) and an Agilent Zorbax Eclipse Plus C18 column (5 μm, 250 mm× 4.6 mm). For ITZ, the mobile phase employed was a mixture of 60% acetonitrile (ACN) and 40% 10 mM ammonium acetate buffer (pH=5.7).[31] For SUB, the mobile phase consisted of 90% ACN and 10% ultrapure water. A 10 μL aliquot of each sample solution was injected and ran at a flow rate of 1 mL/min at room temperature. The detection wavelength was 261 nm and 210 nm for ITZ and SUB, respectively.

### 2.5. Differential Scanning Calorimetry (DSC)

Thermograms were generated through a differential scanning calorimeter (Q1000, TA, DE, USA), using nitrogen as the purge gas at a flow rate of 20 mL/min. Pure indium was used prior to the analysis to calibrate the enthalpy and cell constant. Accurately weighed samples (3–5 mg) were hermetically sealed in aluminum pans, with a pinhole-vented lid if required, and heated from 30 °C to 250 °C at a scanning rate of 10 °C/min. The heating rate of 2 °C/min was applied for constructing the temperature-composition phase diagram while other conditions were unchanged.

### 2.6. Powder X-Ray Diffraction (PXRD)

The X-ray powder diffraction data were collected using a MiniFlex 600 diffractometer (Rigaku, Tokyo, Japan) equipped with Cu-Kα radiation (40kV and 15mA). Samples were uniformly packed in a glass capillary and scanned over the 2θ interval of 3° to 50° at 0.02° step size with scanning speed of 4° per minute.

### 2.7. Fourier-Transform Infrared (FTIR) Spectroscopy

The FTIR spectra were obtained with an FTIR spectrophotometer (ALPHA, Bruker, Germany) in diffuse reflectance mode. A trace amount of the sample was gently mixed with potassium bromide (KBr) using a marble pestle and mortar and then compressed into a thin disc under two tons of force using Mini-Pellet Press (Specac Limited, UK). A total of 16 scans were performed in the range of 4,000 $cm^{-1}$ to 500 $cm^{-1}$ at a resolution of 4 $cm^{-1}$ for each sample.

### 2.8. Spray Drying

Equimolar amounts (0.425 mmol) of ITZ (100 mg) and SUB (24.69 mg) were dissolved in 100 mL mixture of EtOH and CFM (4:1 v/v). Subsequently, the solution was spray-dried using a laboratory scale spray dryer with a high-performance cyclone in suction mode and closed loop configuration (Mini Spray Dryer B-290, Dehumidifier B-296 and Inert Loop B-295; Büchi Labortechnik, Flawil, Switzerland) with nitrogen as the drying gas. Various solute concentrations and compressed gas atomization flow rate were tested (Table 1), while other operating parameters were fixed: inlet temperature of 65 °C, rate of aspiration at 100% (approx. 35 $m^3/h$), solution feed rate of 1.5 mL/min. The outlet temperature was approximately 50 °C.

### 2.9. *In Vitro* Aerosol Performance

The *in vitro* aerosol performance of spray-dried formulations was evaluated using a Next Generation Impactor (NGI; Copley Scientific Limited, Nottingham, UK). Prior to dispersion, a thin layer of silicon grease (Slipicone; DC Products, Waverley, VIC, Australia) was sprayed onto the impactor stages to minimize particle bounce. Approximately 5 mg of each powder was loaded in a Size 3 hydroxypropyl methylcellulose (HPMC) capsule (Capsugel, West Ryde, NSW, Australia), which was then placed in a Breezhaler (Novartis Pharmaceuticals, Hong Kong). Subsequently, the powders were dispersed at a flow rate of 90 mL/min for 2.7 s. After dispersion, the powders remained in the capsule, deposited at the throat, as well as those on the different NGI stages were collected by rinsing with analytical grade ACN, while the inhaler and the adaptor were washed with ultrapure water, followed by dilution with ACN to a final ACN/water (60:40 v/v) solution. Then, the solutions were filtered by 0.45 μm nylon syringe filters and assayed by HPLC. The recovered dose was defined as the sum of powder mass assayed on all the parts in a single run. The emitted fraction (EF) referred to the fraction of powder that exited the inhaler to the total recovered dose. The fine particle fraction (FPF) was the mass fraction of the particles < 5 μm with respect to the recovered dose. The mass median aerodynamic diameter (MMAD) and the geometric standard deviation (GSD) were obtained by a linear fit of cumulative mass vs. log cut-off diameter according to the British Pharmacopoeia (2019).[13]

### 2.10. Scanning Electron Microscopy (SEM)

The particle morphology of the samples was observed by field emission scanning electron microscopy (Hitachi S-4800 FEG, Hitachi, Tokyo, Japan). The powders were sprinkled onto carbon adhesive tape mounted on SEM stubs and sputter coated with approximately 11 nm gold-palladium alloy in two cycles to create a conductive layer and avoid overheating.

### 2.11. Dissolution Test

The dissolution test was conducted in triplicates using the Copley Dissolution Tester DIS8000 (Copley Scientific Limited, Nottingham, UK). For ITZ-SUB cocrystals prepared by rotary evaporation, 100 mg ITZ powders and 124.7 mg ITZ-SUB cocrystal

powders with particle sizes ranging from 125-180 $\mu$m (VWR International, New York, USA) were directly poured into 900 mL of 0.1N HCl solution, with a paddle rotated at 100 rpm, for a period of 180 min at 37 °C. At designated time points of 5, 15, 30, 45, 60, 90, 120 and 180 min, 5 mL of the dissolution medium was withdrawn and replaced with an equal volume of fresh medium. The sample solution was filtered through 0.45 μm nylon syringe filters and assayed for drug content by HPLC method as described in section 2.3.

To investigate the dissolution profile of spray dried ITZ-SUB powders on a DPI respirable fraction, the powders with aerodynamic diameters < 5 μm were collected using a Fast Screening Impactor (FSI; MSP Corporation, Shoreview, USA).[22] Briefly, 10 mg spray dried ITZ-SUB powders were loaded in a Size 3 HPMC capsule and dispersed at 100 L/min flow rate for 2.4 s. After dispersion, powders with aerodynamic diameters < 5 μm were deposited on a glass fiber filter (ADVANTEC; Toyo Roshi Kaisha, Ltd., Japan), then transferred to a watch glass placed in the bottom of the vessel containing 400 mL 0.1 N HCL with 0.3% sodium dodecyl sulfate (SDS),[25, 32] with a paddle stirring at 75 rpm for a period of 180 min at 37 °C. For raw ITZ powders, the amount equivalent to the ITZ mass of the spray-dried ITZ-SUB powders obtained from FSI was directly weighted onto the glass fiber filter attached to the watch glass. The sampling and assay procedures were the same as the previous dissolution test.

### 2.12. Dynamic Vapor Sorption (DVS)

Water sorption isotherms of the samples were obtained using an automated vapor sorption analyzer (Intrinsic DVS, Surface Measurement Systems Ltd., Allentown, PA) at 25 °C and a nitrogen flow of 50 mL/min. Each sample (6-10 mg) was first purged with dry nitrogen until a constant weight was obtained. Then, the sample was exposed to a series of relative humidities (RH) from 0% to 95% with a step size of 5% RH. The RH was changed to the next target value once the equilibrium was reached, where either dm/dt was ≤0.002% with a minimum equilibration time of 0.5 h or maximum equilibration time of 6 h at each specific RH.

### 2.13. Thermal Stress Study

Raw ITZ, raw SUB, ITZ-SUB cocrystal and spray dried ITZ-SUB powders were

put in screw-capped glass bottles separately and then placed in 60 °C oven. After 1 month, samples were collected for PXRD and DSC analysis.

### 2.14. Statistical Analysis

Two-sample *t*-test was employed for data analysis. A p-value less than 0.05 was considered as statistically significant.

## 3. Results and Discussion

### 3.1. Cocrystallization of Itraconazole with Suberic Acid

In a previous study, the cocrystal formation potential of ITZ with a series of structurally similar aliphatic dicarboxylic acids has been established.[26] ITZ cocrystals with C2-C7 dicarboxylic acids could all be obtained by the means of either slow evaporation of a solution in 1:1 THF and CFM mixture or solvent-assisted milling using acetone. However, ITZ failed to cocrystallize with SUB and other longer chain acids. Hence, C7 was believed to be the maximum carbon atom number of the aliphatic chain for successful cocrystallization reaction between ITZ and a dicarboxylic acid.[27] Indeed, only characteristic peaks of ITZ and SUB were found in the PXRD pattern of the samples prepared from the slow evaporation method (Figure 2), indicating the failure of ITZ-SUB cocrystal formation. This was attributed to either the inherent thermodynamically unstable nature of ITZ-SUB or a lower molecular mobility of the longer aliphatic chain.[30] Encouraged by our earlier success, [5] we sought to prepare this elusive ITZ-SUB cocrystal using a rapid solvent removal method, i.e., rotary evaporation.

Although solutions of incongruently saturating systems can generate pure cocrystals by rapid solvent evaporation, it has been suggested by ternary solubility phase diagram that the solubility difference between the cocrystal formers should not be too large in the chosen solvent system because this would significantly alter the propensity of cocrystal formation.[7, 11, 33] Among the tested three pure organic solvents, SUB is much more soluble in THF and EtOH (2728.35 mmol/L and 498.81 mmol/L respectively) than ITZ (37.84 mmol/L and 0.34 mmol/L respectively), while CFM solubility of ITZ (634.83 mmol/L) is much higher than SUB (6.20 mmol/L) (Table 2). While there is no single

solvent system that gives congruent solubility between ITZ and SUB, the EtOH and CFM mixture in 4:1 v/v ratio did yield similar solubilities of ITZ and SUB. The solubility of ITZ detected was 16.07 mmol/L and that of SUB was 16.35 mmol/L, which were not significantly different ($p = 0.61$).

In this study, the cocrystal of ITZ and SUB in 1:1 stoichiometric ratio was successfully obtained from a mixture of EtOH and CFM (4:1) using rotary evaporation. To the best of our knowledge, this is the first 1:1 cocrystal of ITZ with a dicarboxylic acid but without any solvent or water in the crystal lattice. The PXRD pattern of the prepared sample exhibits a series of distinct diffraction peaks ($2\theta = 3.99°$, 6.19°, 9.23°, 12.96°, 18.62° and 21.71°) while characteristic peaks corresponding to ITZ ($2\theta = 14.50°$, 20.42° and 23.54°) and SUB ($2\theta = 9.9°$, 21.34° and 24.77°) were absent (Figure 2). Those unique diffraction peaks of the prepared sample suggested the formation of a new crystalline phase, likely the ITZ-SUB cocrystal, whereas the absence of characteristic peaks of ITZ and SUB denotes the absence of ITZ and SUB in the sample.

Regarding thermal property, the DSC thermogram of the ITZ-SUB cocrystal showed a sharp endothermic peak at 135.7 °C, which is lower than the melting points of ITZ (167.7 °C) and SUB (141.8 °C) (Figure 3). Interestingly, the thermal curve of SUB exhibited another smaller endothermic peak adjacent to the actual melting point, consistent with the previous reports.[34, 35] The enthalpy change of fusion ($\Delta H_f$) of the cocrystal (89.05 kJ/mol) was significantly higher than those of ITZ (79.70 kJ/mol) and SUB (49.94 kJ/mol), demonstrating a stronger crystal lattice upon the cocrystal formation. To further verify the formation of a new cocrystal phase and confirm its stoichiometry, a temperature-composition phase diagram of the ITZ-SUB system was constructed using binary mixtures of SUB with varying ITZ mole fractions from 0 to 1, through DSC analysis (Figure 4). The binary mixtures were generated by rotary evaporation which was the same method as the cocrystal preparation. The phase diagram showed a typical shape of a binary cocrystal system, where three local melting point maxima are separated by two eutectics. It revealed a congruent melting temperature at 50:50 molar composition of either cocrystal former, confirming a 1:1 stoichiometry. Two eutectic points were observed at 0.2 and 0.54 ITZ

mole fractions with melting temperatures at 121.5 °C and 130.2 °C, respectively (Figure 4).

Fourier-transform infrared spectroscopy was conducted to gain an insight into the intermolecular interactions between ITZ and SUB. An outstanding observation when comparing these FTIR spectra is that the C=O stretching vibration of SUB at 1695 $cm^{-1}$ wavelength dramatically shifted to a higher wavelength of 1711 $cm^{-1}$ in the ITZ-SUB spectrum (Figure 5). This can happen if the -OH of the carboxyl group became involved in intermolecular hydrogen bond formation, thus decreasing the intramolecular hydrogen bonding strength between C=O and -OH.[36] In addition, the broad peak corresponding to the O-H group in SUB, covering a wavelength range from 3300 $cm^{-1}$ to 3750 $cm^{-1}$, became narrower at 3425 $cm^{-1}$ in the ITZ-SUB spectrum. Besides, ITZ-SUB cocrystal shared highly similar PXRD pattern with the previously reported ITZ-succinic acid cocrystal in the 2θ range of 3° to 10°.[28] These results imply that the carboxyl groups of SUB and the nitrogen atoms to the 1,2,4-triazole group of ITZ participated in the formation of hydrogen bond, which is an interaction observed in the ITZ cocrystal with succinic acid.[28]

Here, rapid rotary evaporation technique was again proven to be effective in the fabrication of an elusive cocrystal. Suspending ITZ-SUB in water led to dissociation and formation of ITZ. Thus, the formation of the ITZ-SUB cocrystal is likely realized by kinetic entrapment as suggested by Ostwald's rule of stages[37], where thermodynamically unstable phases appear first during the crystallization from solutions. However, the cocrystal powders prepared by rotary evaporation technique were not suitable for pulmonary drug delivery as the particle size was larger than 100 $\mu$m (Figure S1). Hence, spray drying was employed to produce smaller ITZ-SUB particles.

### 3.2.Spray Dried ITZ-SUB powders

Having proven the feasibility of preparing the ITZ-SUB cocrystal by fast solvent removal through rotary evaporation, spray drying was further probed for the feasibility of producing inhalable ITZ-SUB dry powder formulations with suitable aerosol performance. Spray drying is a versatile technique that allows continuous production of dry powders, which can fit diverse purposes by adjusting the feed solution/suspension composition and various process parameters. In this study, feed solute concentration and compressed gas

atomization flow rate were selected for process optimization because of their proven impact on the particle size, where particle size generally increases with increasing solute concentration and/or decreasing compressed gas atomization flow rate.[8-10, 38]

Among the six tested spray-dried formulations (Table 1), SD3 appeared to be ideal for pulmonary delivery as it exhibited the most desirable MMAD and GSD ($2.56 \pm 2.27$ $\mu$m) as well as the highest FPF (64.1% w/w), which was much higher than that of most commercial products (around 30% w/w).[39] As mentioned above, aerodynamic diameters of 1-5 $\mu$m are widely accepted for drug delivery to the lung, but the range from 1 to 3 $\mu$m is preferred for reaching the deep lung region.[14, 15] This size range correlates well with good clinical response to local treatment of lung diseases, such as IPA, and favors the penetration of the drug into the capillary-rich alveolar region for systemic treatment. Additionally, since SD3 can be delivered to deep lung without using a carrier, blend uniformity problems are eliminated.[40] A carrier-free formulation also allows the delivery of high dose ITZ to the lung since the carrier typically occupies 67.5% of the formulation mass.[41]

Both solute concentration of the feed solution and the compressed gas atomization flow rate did affect the $d_A$ of the resulted formulations. The primary particle size decreased with decreasing solute concentration and increasing of the gas atomization flow rate (Figure S5), as expected.[8-10, 38] However, smaller primary particles are more likely to aggregate. Therefore, a lower solute concentration and a higher gas flow rate did not necessarily generate a formulation with smaller $d_A$upon aerosolization.

The NGI dispersion plot revealed that 68% of the SD3 powder deposited on Stages 3-5, where the aerodynamic diameters fell within 3.61-0.76 $\mu$m (Figure 6). However, SD3 powder consisted of agglomerates of smooth spherical particles with diameter around 1 $\mu$m (Figure 7). The particles deposited on the different stages of the NGI mainly differ in the extent of agglomeration instead of primary particle size (Figure S7). Upon inhalation, the spray-dried ITZ-SUB cohesive powder formed smaller agglomerates, favoring the deposition in the lower lung region. The primary submicron particles may potentially penetrate into the deep lung after the agglomerates have settled and de-agglomerated. Besides, the electrostatic nature of these agglomerates may lead to a more efficient deposition via the electrostatic attraction between the particle and the induced opposite

charge on the wall of the lung.[42] Furthermore, in comparison with particles of the same size, the agglomerates usually has a better bioavailability. This is due to the larger surface area of its rough surface, thus enhancing dissolution rate, delaying lung clearance, and improving systemic absorption.[43]

It is worth noting that besides the most commonly occurring smooth spheres,[10] there are also a few rod-shaped particles present in the spray dried powders, indicating the possibility of crystallized ITZ-SUB. The PXRD pattern of SD3 indicated low crystallinity, but the characteristic peaks of ITZ-SUB at 6.19°, 9.23° and 21.71° were still observed (Figure 2), while other spray dried powders were largely amorphous (Figure S2). The DSC thermogram of all the spray dried samples illustrated the glass transition of the amorphous content at around 50 °C, followed by the evaporation of the residual solvent and a broad crystallization exotherm (Figure S3). Eventually, the recrystallized ITZ-SUB cocrystals melted at 135.7 °C (Figure 3). The FTIR spectra of all the spray dried powders also exhibited similar peaks with ITZ-SUB cocrystals (Figure 5 & S4). Hence, it can be concluded that the spray dried powders contained mainly co-amorphous ITZ-SUB, but a small portion of cocrystals still exists. Albeit the drug particles are generally required to be crystalline due to the stability issue, the amorphous form is considered to be superior for its rapid dissolution and absorption.[44]

### 3.3. Dissolution Profile

As ITZ belongs to BCS Class II, its therapeutic efficacy is limited by its solubility. It has been shown that the solubility of poorly-water soluble drugs can be improved by cocrystallization, especially when using a water-soluble coformer.[45, 46] However, direct measurement of ITZ-SUB aqueous solubility was not possible as the cocrystal underwent dissociation when suspended in an aqueous solution owing to the thermodynamically unstable nature of the cocrystals. In the contrary, dissolution test is a useful alternative for solubility measurement. Considering ITZ is commercially available as oral tablet and capsule formulations, we have assessed the dissolution performance of both oral ITZ-SUB cocrystal prepared by rotary evaporation for possible use in oral tablets or capsules and the spray-dried inhalable ITZ-SUB cocrystal agglomerates.

The dissolution of crystalline ITZ-SUB prepared by rotary evaporation was tested in a 0.1N HCl solution to stimulate the gastric environment. To minimize the size, size distribution and morphology effects of the particles, only the 125- 180 $\mu$m fraction of both raw ITZ and ITZ-SUB cocrystals was used for the test. The dissolution profile of the raw ITZ plateaued at lower than 6%, while ITZ-SUB cocrystals followed first-order kinetics with approximately 80% ITZ dissolved after 180 min (Figure 8). The intrinsic dissolution rate (IDR) can be determined by the equation: $IDR = (dm/dt)_{max}/A$, where $(dm/dt)_{max}$ is the slope of the initial linear region of the cumulative dissolution curve and $A$ is the specific surface area of the dissolution sample.[47] Although the exact specific surface area of the samples was not measured in this study, the sieved ITZ-SUB cocrystal and raw ITZ were within the same size range (125-180 $\mu$m) as well as exhibiting similar particle morphology (Figure S8). Hence, the IDR ratio of ITZ-SUB to ITZ can be roughly estimated by the ratio of the slope, which is 39.2, suggesting roughly 39-fold faster in the rate of dissolution of the ITZ-SUB cocrystal than raw ITZ in 0.1 N HCl. Concerning the fraction of release, significantly more ITZ-SUB cocrystal was dissolved than raw ITZ (66.8% and 2.1%, respectively; $p = 8.2\times10^{-5}$ ) at 90 min, which was the end point of ITZ dissolution test recommended by US FDA.[48] In addition, the apparent solubility, measured one day after the dissolution test, of 97.1 $\mu$g/mL for ITZ-SUB cocrystal was significantly higher than 0.6 $\mu$g/mL for raw ITZ ($p = 5 \times 10^{-8}$).

Hence, cocrystallization of ITZ with SUB remarkably improved the dissolution performance and the apparent solubility of ITZ in an acidic medium. This substantial amelioration can be attributed to the high aqueous solubility of SUB.[46] The dissolution rate of dry powder inhaler formulations is also critical as undissolved particles will be cleared by macrophage phagocytosis in the alveolar region and the mucociliary escalator in the conducting airways.[44] Considering this, the dissolution protocol of dry powder inhaler formulations must be different from that of conventional solid dosage forms as only particles with MMAD < 5μm could effectively enter the lower airways. Nevertheless, no pharmacopoeia method or universally acceptable protocol has yet been developed for DPI formulation. To this end, an FSI was employed in this study to collect particles with MMAD < 5μm.[22] Before the dissolution test, the FPF of spray-dried ITZ-SUB powders using FSI, assayed by HPLC, was 64.6%. Here, we utilized a 0.1 N HCl with 0.3% SDS

as the medium in this dissolution test because previous studies have substantiated its close correlation with the *in vivo* study that qualitatively compared different aerosol formulations in the lung.[24, 25, 49] The presence of SDS is expected to improve the dissolution performance of the raw ITZ by improving wetting, provided no insoluble complex is formed with ITZ.[50] However, raw ITZ still dissolved slowly and only 50% was dissolved after 180 min. On the contrary, the spray dried ITZ-SUB powders with $d_A$ < 5 $\mu$m dissolved very rapidly in the initial 15 min and reached a plateau at 80% ITZ fraction of release after 30 min (Figure 9). At 180 min, the fraction of ITZ dissolved in ITZ-SUB was significantly higher than raw ITZ ($p = 0.03$). Therefore, the spray dried ITZ-SUB cocrystals substantially enhanced both the dissolution rate as well as the extent of ITZ dissolved, which can be explained by both the amorphous nature and the large specific surface area of the agglomerate structure. Consequently, the spray-dried ITZ-SUB holds promise for pulmonary administration of ITZ.

### 3.4. Stability Profile

Stability is a key consideration in the development of pharmaceutical products. Generally, relative humidity stress study and thermal stress study are the most common approaches for stability test. As indicated by the DVS results, none of the crystalline materials adsorbed a significant amount of water (< 0.5%) at 95% RH (Figure 10). Therefore, ITZ, SUB and ITZ-SUB cocrystal are all non-hygroscopic. However, both spray dried ITZ and ITZ-SUB exhibited higher moisture sorption but the amounts were not significant as the weight only changed less than 2.5%. Compared with spray dried ITZ which was completely amorphous, spray dried ITZ-SUB powders adsorbed a less amount of water. For the stability under thermal stress, ITZ-SUB prepared by both rotary evaporation and spray drying did not dissociate into individual components at 60 $^{o}$C for 1 month. The characteristic peaks of the cocrystal in the PXRD pattern were still evident and the melting point remained unchanged according to the DSC thermogram (Figure 11). While amorphous form of a chemical compound is generally considered less stable than its crystalline counterpart, the spray dried ITZ-SUB powders did not undergo significant crystallization after 1-month storage at 60 °C according to PXRD pattern (Figure 11d). The residual solvent in the spray-dried ITZ-SUB was removed during storage as indicated

by the flat baseline before the melting point in its DSC thermogram. This suggests that residual solvent can be easily removed from the spray-dried ITZ-SUB in commercial manufacturing. Although a crystallization exotherm is absent, a melting event at 135.7 °C corresponding to that of ITZ-SUB crystal is clearly observed. Thus, any crystallization must have occurred over a wide temperature range so that only a broad peak can be expected. It is worth to mention that ITZ in its branded product, Sporanox®, also exists in an amorphous state.[17] Hence, the stability issue should not hinder the commercialization of spray dried ITZ-SUB.

## 4. Conclusion

In this study, a phase pure ITZ-SUB 1:1 cocrystal was successfully prepared by rapid solvent removal using rotary evaporation, and characterized by a variety of techniques including PXRD, DSC, and FTIR. Despite the markedly improved dissolution performance, the size of the resulting cocrystal restricted its application in the development of inhalable formulations. To this end, spray drying was further employed to fabricate ITZ-SUB agglomerates for superior pulmonary delivery. The spray dried ITZ-SUB powders possessed more desirable size distribution, morphology, and dissolution rate for inhalation in comparison to the parent drug.

## Acknowledgments

We thank financial supports from The University of Hong Kong (Project number: 104004777 and 204600519). We also thank Ms. Roshni Dattani (School of Pharmacy, University College London) for assistance with the dissolution study.

## Supporting Information

PXRD patterns, DSC profiles, FTIR spectra, SEM images and NGI dispersion data of spray dried ITZ-SUB, SEM images of spray dried ITZ-SUB powders (SD3) deposited on the throat and different stages of the NGI, SEM images of ITZ and ITZ-SUB cocrystal.

## References


1. Schultheiss, N.; Newman, A., Pharmaceutical cocrystals and their physicochemical properties. *Cryst. Growth Des.* **2009**, *9*, 2950-2967.

2. Karki, S.; Friščić, T.; Fábián, L.; Laity, P. R.; Day, G. M.; Jones, W., Improving mechanical properties of crystalline solids by cocrystal formation: new compressible forms of paracetamol. *Adv. Mater.* **2009,** *21*, 3905-3909.

3. FDA, U. S., Regulatory Classification of Pharmaceutical Co-Crystals Guidance for Industry. Revision 1 ed.; Washington, DC. **2018**.

4. Jones, W.; Motherwell, W. S.; Trask, A. V., Pharmaceutical cocrystals: an emerging approach to physical property enhancement. *MRS Bull.* **2006,** *31*, 875-879.

5. Chow, S. F.; Shi, L.; Ng, W. W.; Leung, K. H. Y.; Nagapudi, K.; Sun, C. C.; Chow, A. H., Kinetic entrapment of a hidden curcumin cocrystal with phloroglucinol. *Cryst. Growth Des.* **2014**, *14*, 5079-5089.

6. Wong, S. N.; Hu, S.; Ng, W. W.; Xu, X.; Lai, K. L.; Lee, W. Y. T.; Chow, A. H. L.; Sun, C. C.; Chow, S. F., Cocrystallization of curcumin with benzenediols and benzenetriols via rapid solvent removal. *Cryst. Growth Des.* **2018**, *18*, 5534-5546.

7. Vehring, R., Pharmaceutical particle engineering via spray drying. Pharm. Res. 2008, 25 (5), 999-1022.

8. Nandiyanto, A. B. D.; Okuyama, K., Progress in developing spray-drying methods for the production of controlled morphology particles: From the nanometer to submicrometer size ranges. *Adv. Powder Technol.* **2011**, *22*, 1-19.

9. Paudel, A.; Worku, Z. A.; Meeus, J.; Guns, S.; Van den Mooter, G., Manufacturing of solid dispersions of poorly water soluble drugs by spray drying: formulation and process considerations. *Int. J. Pharm.* **2013**, *453*, 253-284.

10. Vicente, J.; Pinto, J.; Menezes, J.; Gaspar, F., Fundamental analysis of particle formation in spray drying. *Powder Technol.* **2013**, *247*, 1-7.

11. Alhalaweh, A.; Velaga, S., Formation of cocrystals from stoichiometric solutions of incongruently saturating systems by spray drying. *Cryst. Growth Des.* **2010**, *10*, 3302-3305.

12. Alhalaweh, A.; Kaialy, W.; Buckton, G.; Gill, H.; Nokhodchi, A.; Velaga, S. P., Theophylline cocrystals prepared by spray drying: physicochemical properties and aerosolization performance. *AAPS PharmSciTech* **2013**, *14* , 265-276.

13. Medicines & Healthcare products Regulatory Agency, British Pharmacopoeia. **2019**.

14. Stahlhofen, W.; Gebhart, J.; Heyder, J., Experimental determination of the regional deposition of aerosol particles in the human respiratory tract. *Am. Ind. Hyg. Assoc. J.* **1980**, *41*, 385-398a.

15. Yang, W.; Peters, J. I.; Williams III, R. O., Inhaled nanoparticles—a current review. *Int. J. Pharm.* **2008**, *356*, 239-247.

16. Janssen Pharmaceuticals, I., U.S. Package Insert - SPORANOX. FDA, U. S., Ed. **2018**.

17. Maghrabi, F.; Denning, D. W., The Management of Chronic Pulmonary Aspergillosis: The UK National Aspergillosis Centre Approach. *Curr Fungal Infect Rep* **2017**, *11*, 242-251.

18. Davies, G.; Rolle, A.-M.; Maurer, A.; Spycher, P. R.; Schillinger, C.; Solouk-Saran, D.; Hasenberg, M.; Weski, J.; Fonslet, J.; Dubois, A., Towards translational ImmunoPET/MR imaging of invasive pulmonary aspergillosis: the humanised monoclonal antibody JF5 detects Aspergillus lung infections in vivo. *Theranostics.* **2017**, *7*, 3398.

19. Aftab, B. T.; Dobromilskaya, I.; Liu, J. O.; Rudin, C. M., Itraconazole inhibits angiogenesis and tumor growth in non–small cell lung cancer. *Cancer Res.* **2011**, *71*, 6764-6772.

20. Antonarakis, E. S.; Heath, E. I.; Smith, D. C.; Rathkopf, D.; Blackford, A. L.; Danila, D. C.; King, S.; Frost, A.; Ajiboye, A. S.; Zhao, M., Repurposing itraconazole as a treatment for advanced prostate cancer: a noncomparative randomized phase II trial in men with metastatic castration-resistant prostate cancer. *Oncologist* **2013,** *18*, 163-173.

21. Rudin, C. M.; Brahmer, J. R.; Juergens, R. A.; Hann, C. L.; Ettinger, D. S.; Sebree, R.; Smith, R.; Aftab, B. T.; Huang, P.; Liu, J. O., Phase 2 study of pemetrexed and itraconazole as second-line therapy for metastatic nonsquamous non–small-cell lung cancer. *J. Thorac. Oncol.* **2013**, *8*, 619-623.

22. Domínguez-Gil Hurlé, A.; Sánchez Navarro, A.; Garcia Sanchez, M., Therapeutic drug monitoring of itraconazole and the relevance of pharmacokinetic interactions. *Clin. Microbiol. Infect.* **2006**, *12*, 97-106.

23. Duret, C.; Merlos, R.; Wauthoz, N.; Sebti, T.; Vanderbist, F.; Amighi, K., Pharmacokinetic evaluation in mice of amorphous itraconazole-based dry powder formulations for inhalation with high bioavailability and extended lung retention. *Eur. J. Pharm. Biopharm.* **2014**, *86*, 46-54.

24. Duret, C.; Wauthoz, N.; Sebti, T.; Vanderbist, F.; Amighi, K., Solid dispersions of itraconazole for inhalation with enhanced dissolution, solubility and dispersion properties. *Int. J. Pharm.* **2012**, *428*, 103-113.

25. McConville, J. T.; Overhoff, K. A.; Sinswat, P.; Vaughn, J. M.; Frei, B. L.; Burgess, D. S.; Talbert, R. L.; Peters, J. I.; Johnston, K. P.; Williams, R. O., Targeted high lung concentrations of itraconazole using nebulized dispersions in a murine model. *Pharm. Res.* **2006**, *23*, 901-911.

26. Shevchenko, A.; Bimbo, L. M.; Miroshnyk, I.; Haarala, J.; Jelínková, K.; Syrjänen, K.; van Veen, B.; Kiesvaara, J.; Santos, H. A.; Yliruusi, J., A new cocrystal and salts of itraconazole: Comparison of solid-state properties, stability and dissolution behavior. *Int. J. Pharm.* **2012**, *436*, 403-409.

27. Shevchenko, A.; Miroshnyk, I.; Pietilä, L.-O.; Haarala, J.; Salmia, J.; Sinervo, K.; Mirza, S.; van Veen, B.; Kolehmainen, E.; Nonappa, J.; Yliruusi, J., Diversity in Itraconazole Cocrystals with Aliphatic Dicarboxylic Acids of Varying Chain Length. . *Cryst. Growth Des.* **2013**, *13*, 4877-4884.

28. Remenar, J. F.; Morissette, S. L.; Peterson, M. L.; Moulton, B.; MacPhee, J. M.; Guzmán, H. R.; Almarsson, Ö., Crystal engineering of novel cocrystals of a triazole drug with 1, 4-dicarboxylic acids. *J. Am. Chem. Soc.* **2003**, *125*, 8456-8457.

29. Espinosa-Lara, J. C.; Guzman-Villanueva, D.; Arenas-García, J. I.; Herrera-Ruiz, D.; Rivera-Islas, J.; Román-Bravo, P.; Morales-Rojas, H.; Höpfl, H., Cocrystals of Active Pharmaceutical Ingredients—Praziquantel in Combination with Oxalic, Malonic, Succinic, Maleic, Fumaric, Glutaric, Adipic, And Pimelic Acids. *Cryst. Growth Des.* **2013**, *13*, 169-185.

30. Sarceviča, I.; Kons, A.; Orola, L., Isoniazid cocrystallisation with dicarboxylic acids: vapochemical, mechanochemical and thermal methods. *CrystEngComm* **2016**, *18*, 1625-1635.

31. Wan, K. Y.; Wong, K. W.; Chow, A. H. L.; Chow, S. F., Impact of molecular rearrangement of amphiphilic stabilizers on physical stability of itraconazole nanoparticles prepared by flash nanoprecipitation. *Int. J. Pharm.* **2018**, *542*, 221-231.

32. Liao, Q.; Yip, L.; Chow, M. Y.; Chow, S. F.; Chan, H.-K.; Kwok, P. C.; Lam, J. K., Porous and highly dispersible voriconazole dry powders produced by spray freeze drying for pulmonary delivery with efficient lung deposition. Int. J. Pharm. **2019**, *560*, 144-154.

33. Childs, S. L.; Rodríguez-Hornedo, N.; Reddy, L. S.; Jayasankar, A.; Maheshwari, C.; McCausland, L.; Shipplett, R.; Stahly, B. C., Screening strategies based on solubility and solution composition generate pharmaceutically acceptable cocrystals of carbamazepine. *CrystEngComm* **2008**, *10*, 856-864.

34. Cingolani, A.; Berchiesi, G., Thermodynamic properties of organic compounds. *J. Therm. Anal.* **1974**, *6*, 87-90.

35. Sailakshmi, G.; Mitra, T.; Sinha, S.; Chatterjee, S.; Gnanamani, A.; Mandal, A., Suberic acid acts as a dissolving agent as well as a crosslinker for natural polymers (carbohydrate and protein): a detailed discussion on the chemistry behind the interaction. *J. Macromol Sci A* **2012**, *49*, 619-629.

36. Nie, B.; Stutzman, J.; Xie, A., A vibrational spectral maker for probing the hydrogen-bonding status of protonated Asp and Glu residues. *Biophys. J.* **2005**, *88*, 2833-2847.

37. Threlfall, T., Structural and thermodynamic explanations of Ostwald's rule. Org. *Process Res. Dev.* **2003**, *7*, 1017-1027.

38. Karashima, M.; Sano, N.; Yamamoto, S.; Arai, Y.; Yamamoto, K.; Amano, N.; Ikeda, Y., Enhanced pulmonary absorption of poorly soluble itraconazole by micronized cocrystal dry powder formulations. *Eur. J. Pharm. Biopharm.* **2017**, *115*, 65-72.

39. Demoly, P.; Hagedoorn, P.; de Boer, A. H.; Frijlink, H. W., The clinical relevance of dry powder inhaler performance for drug delivery. *Respir Med* **2014**, *108*, 1195-1203.

40. Healy, A. M.; Amaro, M. I.; Paluch, K. J.; Tajber, L., Dry powders for oral inhalation free of lactose carrier particles. *Adv. Drug Deliv. Rev.* **2014**, *75*, 32-52.

41. Larhrib, H.; Zeng, X. M.; Martin, G. P.; Marriott, C.; Pritchard, J., The use of different grades of lactose as a carrier for aerosolised salbutamol sulphate. *Int. J. Pharm.* **1999**, *191*, 1-14.

42. Chan, H.-K., Dry powder aerosol delivery systems: current and future research directions. *J. Aerosol Med* **2006**, *19*, 21-27.

43. Kreyling, W. G.; Semmler-Behnke, M.; Möller, W., Ultrafine particle–lung interactions: does size matter? *J. Aerosol Med* **2006**, *19*, 74-83.

44. Chow, A. H.; Tong, H. H.; Chattopadhyay, P.; Shekunov, B. Y., Particle engineering for pulmonary drug delivery. Pharm. Res. **2007**, *24*, 411-437.

45. Babu, N. J.; Nangia, A., Solubility advantage of amorphous drugs and pharmaceutical cocrystals. *Cryst. Growth Des.* **2011**, *11*, 2662-2679.

46. Good, D. J.; Rodriguez-Hornedo, N., Solubility advantage of pharmaceutical cocrystals. *Cryst. Growth Des.* **2009**, *9*, 2252-2264.

47. Noyes, A. A.; Whitney, W. R., The rate of solution of solid substances in their own solutions. *J. Am. Chem. Soc.* 1**897**, *19*, 930-934.

48. FDA, U. S. Dissolution Methods: Itraconazole. **2013**.

49. Huang, Z.; Lin, L.; McGoverin, C.; Liu, H.; Wang, L.; Zhou, Q. T.; Lu, M.; Wu, C., Dry powder inhaler formulations of poorly water-soluble itraconazole: A balance between in-vitro dissolution and in-vivo distribution is necessary. *Int. J. Pharm.* **2018**, *551*, 103-110.

50. Guo, Y.; Wang, C.; Dun, J.; Du, L.; Hawley, M.; Sun, C. C., Mechanism for the reduced dissolution of ritonavir tablets by sodium lauryl sulfate. *J. Pharm. Sci.* **2018**, *108*, 516-524.

**Table 1.** Aerodynamic size distribution (MMAD, GSD and FPF) of spray-dried formulations under different solute concentrations and compressed gas atomization flow rates.

| Formulation | Solute Concentration (mmol/L) | Gas flow (Nl/h) | MMAD ($\mu$m) | GSD ($\mu$m) | FPF (% w/w) |
|---|---|---|---|---|---|
| SD1 | 1.14 | 742 | 4.22 | 3.03 | 33.71 |
| SD2 | 1.14 | 601 | 4.04 | 2.75 | 42.27 |
| SD3 | 3.41 | 742 | 2.56 | 2.27 | 64.10 |
| SD4 | 3.41 | 601 | 3.69 | 2.75 | 42.49 |
| SD5 | 5.68 | 742 | 5.05 | 2.92 | 32.98 |
| SD6 | 5.68 | 601 | 4.49 | 2.87 | 37.2 |

**Table 2.** Solubilities (mean ± standard deviation) of ITZ and SUB in selected organic solvents (n = 3).

| Sample | Solubility (mmol/L) in: | | | |
|---|---|---|---|---|
| | THF | EtOH | CFM | EtOH/CFM (4:1 v/v) |
| ITZ | 37.84±0.34 | 0.34±0.01 | 634.83±7.85 | 16.07±0.57 |
| SUB | 2728.35±33.32 | 498.81±9.83 | 6.20±0.32 | 16.35±0.66 |

**Figure 1.** Chemical structure of (1) ITZ and (2) SUB.

(1)

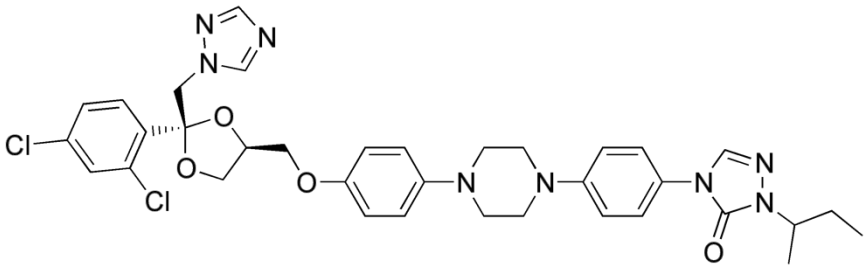

(2)

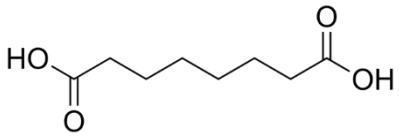

**Figure 2.** PXRD patterns of ITZ, SUB, Samples obtained from slow evaporation, ITZ-SUB cocrystals and spray dried ITZ-SUB (SD3). * denotes the characteristic peaks of ITZ-SUB cocrystal.

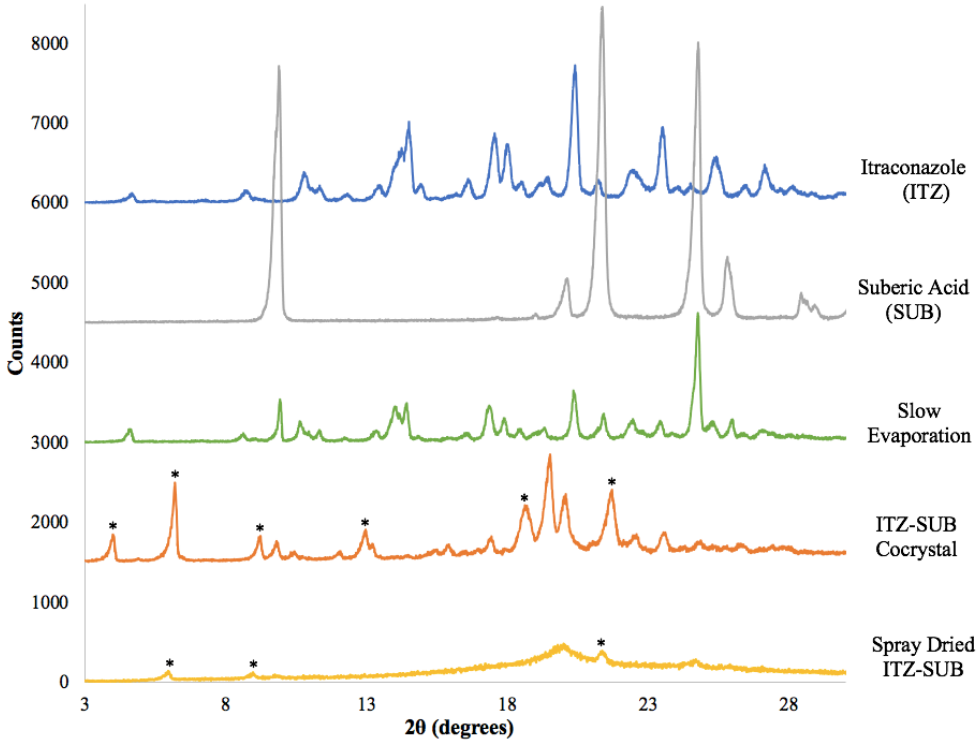

**Figure 3.** DSC profiles of ITZ, SUB, ITZ-SUB cocrystals and spray dried ITZ-SUB (SD3).

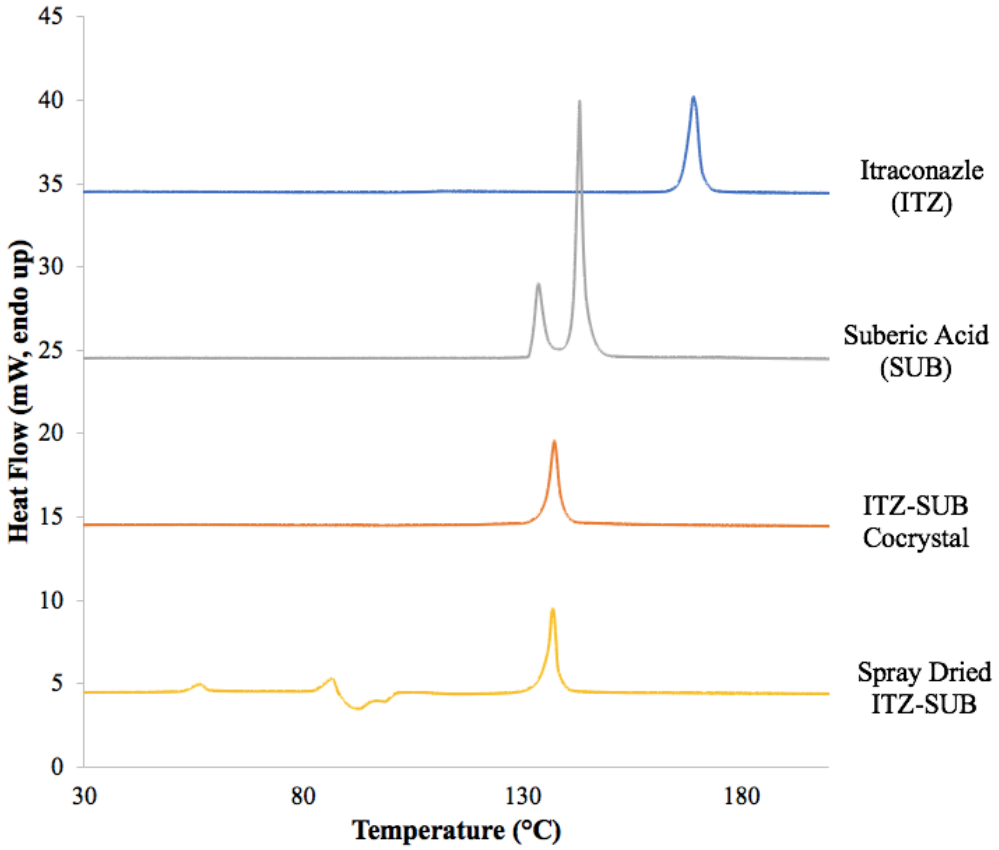


**Figure 4.** Melting point-composition phase diagram of ITZ-SUB cocrystal.

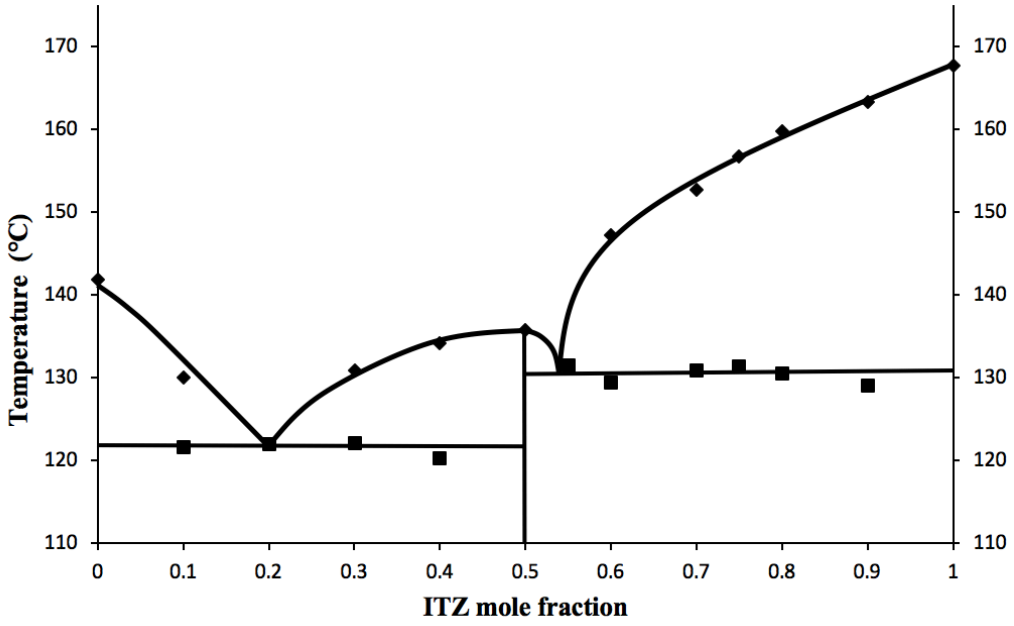

**Figure 5.** FTIR spectra of ITZ, SUB, ITZ-SUB cocrystal and spray dried ITZ-SUB (SD3).

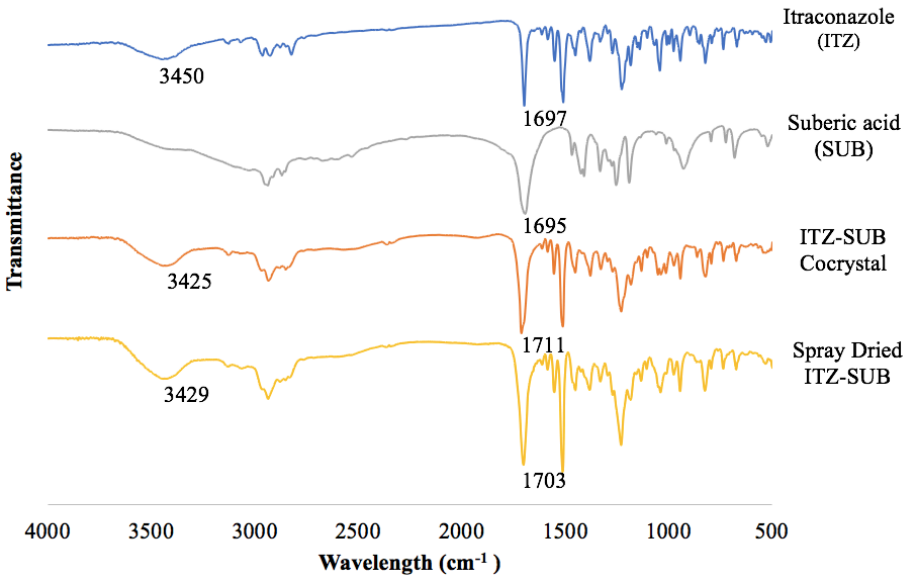


**Figure 6.** NGI dispersion data of spray dried ITZ-SUB (SD3, n=3). S1–S7 presents impactor stages 1–7, followed by the corresponding upper aerodynamic cut-off diameter in parentheses. MOC is the micro-orifice collector in the NGI.

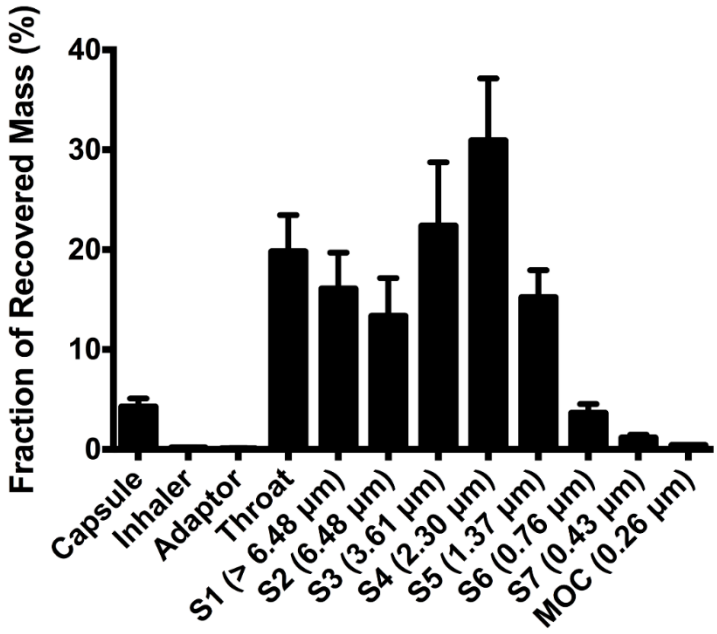

**Figure 7.** SEM images of spray dried ITZ-SUB (SD3). (a) at 500× magnification; (b) at 5000 × magnification.

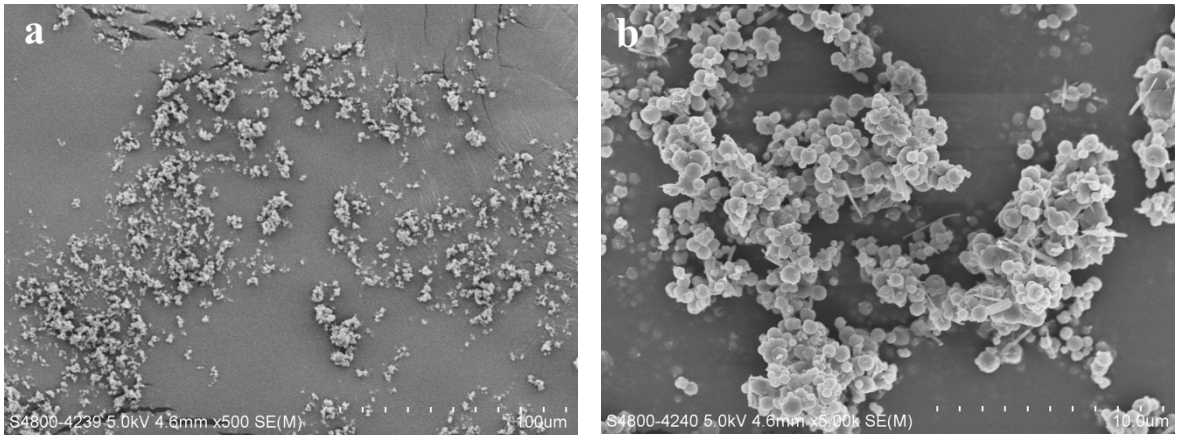


**Figure 8.** Dissolution profiles of ITZ and ITZ-SUB cocrystal with size ranged 125-180 $\mu$m (n=3).

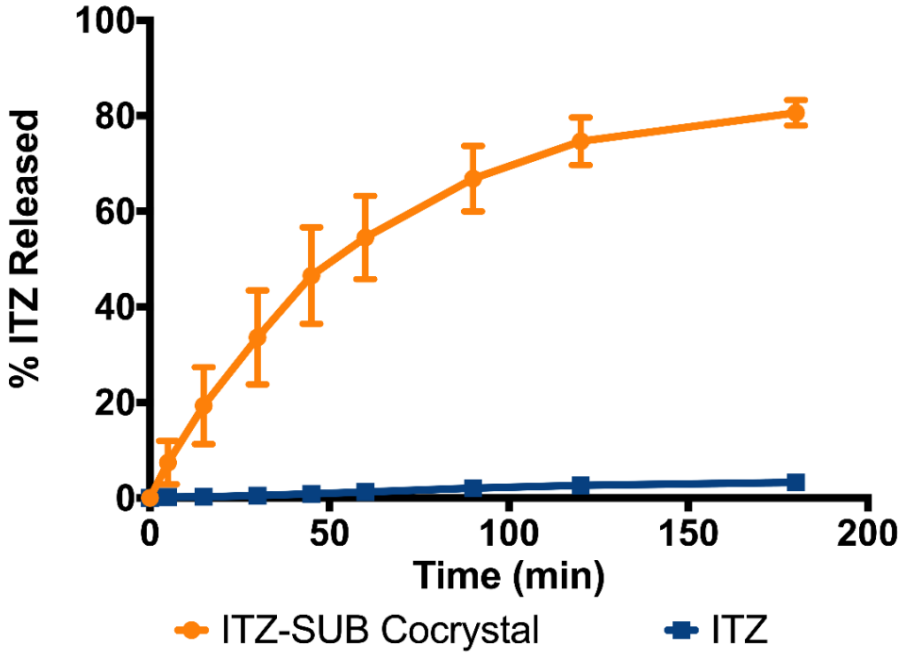

**Figure 9.** Dissolution profiles of ITZ and spray dried ITZ-SUB powders (SD3) with aerodynamic diameters < 5 µm (n=3).

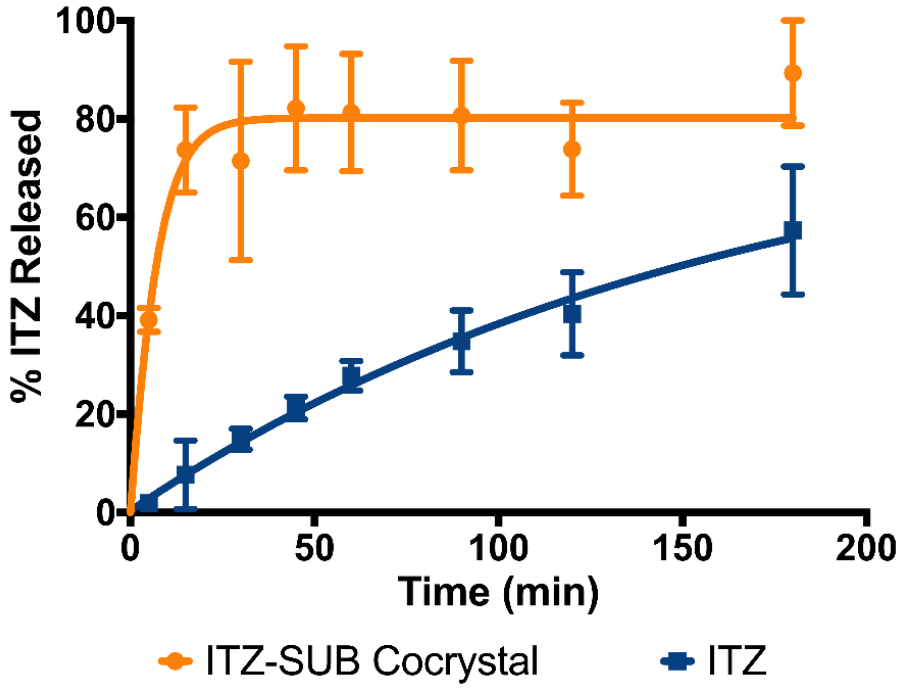


**Figure 10.** Water sorption isotherms at 25 °C of ITZ, SUB, ITZ-SUB cocrystal, SD ITZ and SD ITZ-SUB.

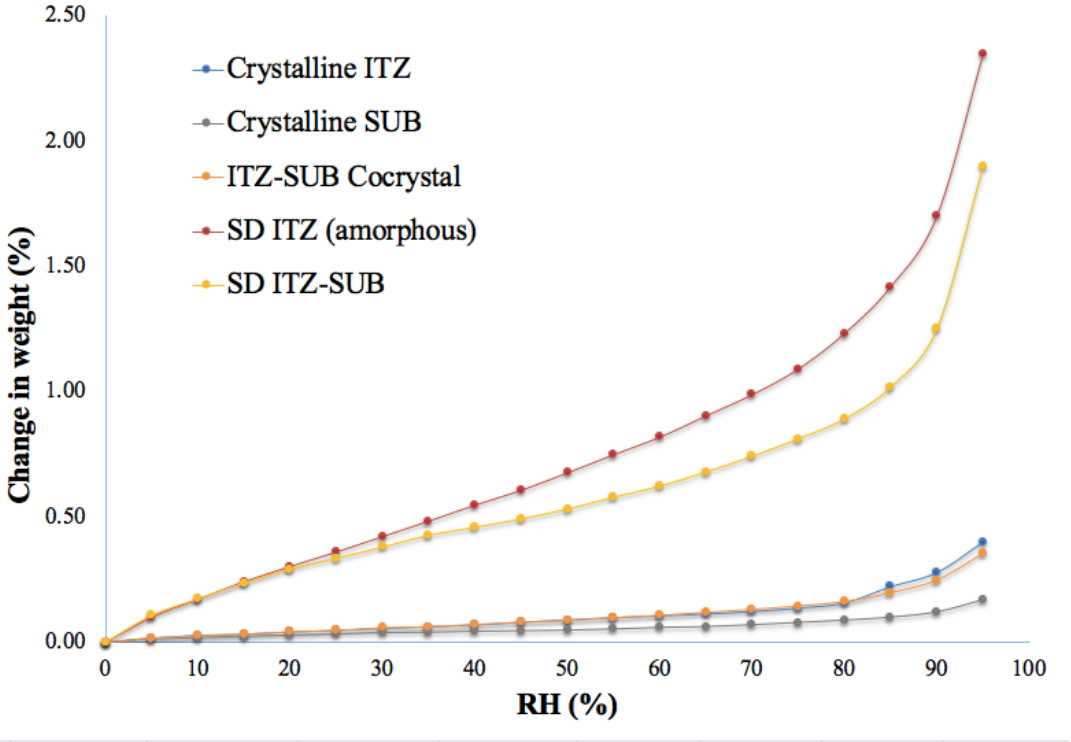

**Figure 11.** Stability profiles of a) ITZ, b) SUB, c) ITZ-SUB cocrystals and d) spray dried ITZ-SUB using PXRD and e) ITZ, f) SUB, g) ITZ-SUB cocrystals and h) spray dried ITZ-SUB using DSC analysis.

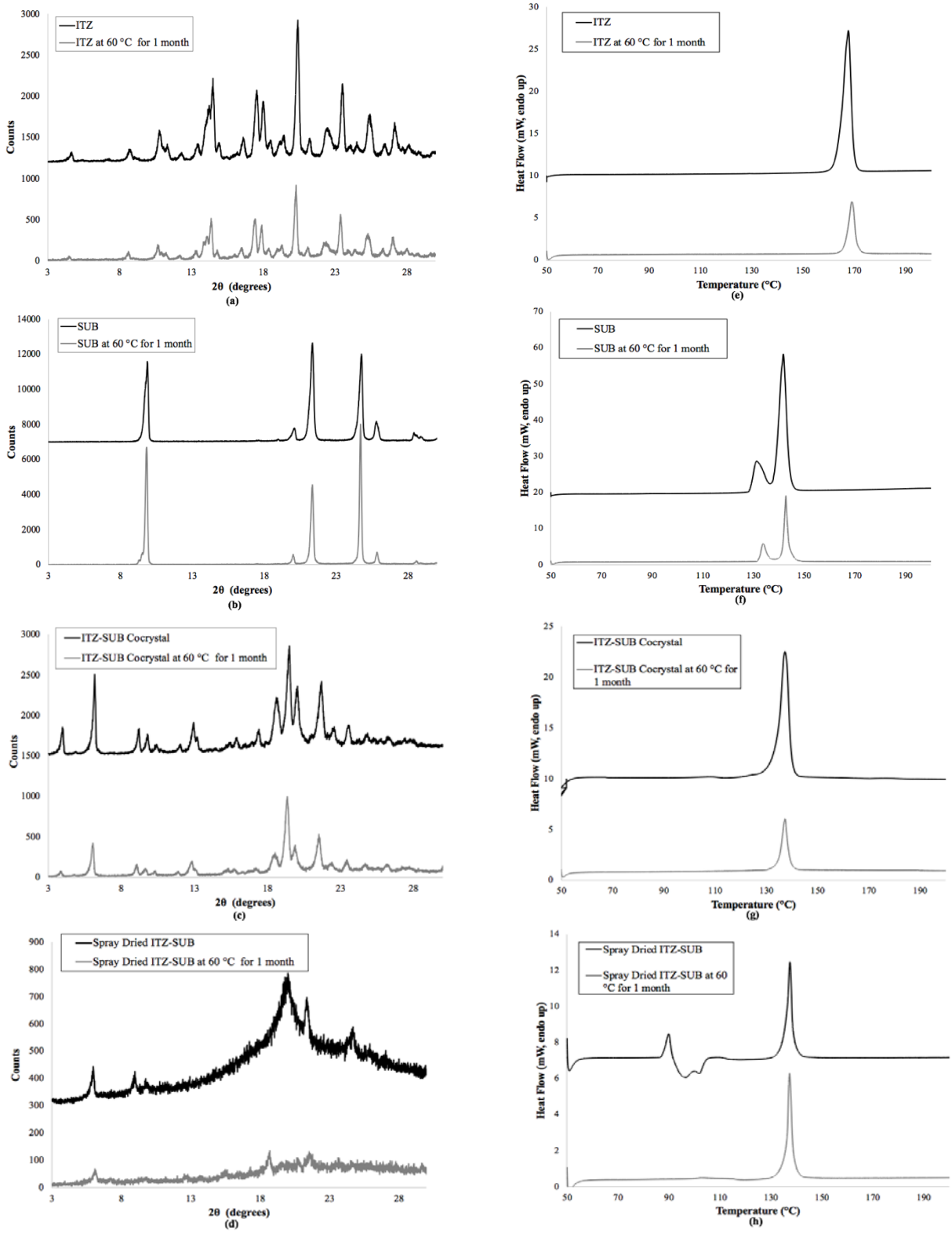

For Table of Contents Use Only,

# Cocrystal Engineering of Itraconazole with Suberic acid via Rotary Evaporation and Spray Drying

Jingwen Weng[1,#], Si Nga Wong[1,#], Xiaoyan Xu[1], Bianfei Xuan[1], Chenguang Wang[2], Ruipeng Chen[3], Changquan Calvin Sun[2], Richard Lakerveld[2], Philip Chi Lip Kwok[3], Shing Fung Chow[1,*]

TOC graphic:

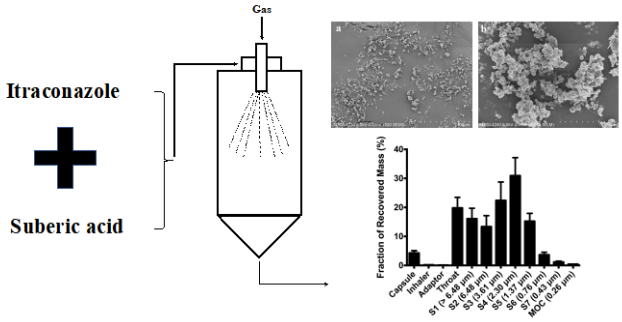


Synopsis:

Using spray drying, we have successfully prepared 1:1 itraconazole-suberic acid agglomerates exhibiting improved dissolution behavior and excellent aerosol performance for deep lung delivery.

**Supporting Information**

# Cocrystal Engineering of Itraconazole with Suberic acid via Rotary Evaporation and Spray Drying

Jingwen Weng[1,#], Si Nga Wong[1,#], Xiaoyan Xu[1], Bianfei Xuan[1], Chenguang Wang[2], Ruipeng Chen[3], Changquan Calvin Sun[2], Richard Lakerveld[3], Philip Chi Lip Kwok[4], Shing Fung Chow[1,*]

[1]Department of Pharmacology and Pharmacy, Li Ka Shing Faculty of Medicine, The University of Hong Kong, Pokfulam, Hong Kong

[2]Pharmaceutical Materials Science and Engineering Laboratory, Department of Pharmaceutics, College of Pharmacy, University of Minnesota, USA

[3]Department of Chemical and Biologic Engineering, The Hong Kong University of Science & Technology, Clear Water Bay, Kowloon, Hong Kong

[4]School of Pharmacy, The University of Sydney, New South Wales, Australia.

# *Equal contribution*

* *Corresponding author*

**Figure S1.** SEM image of ITZ-SUB cocrystal.

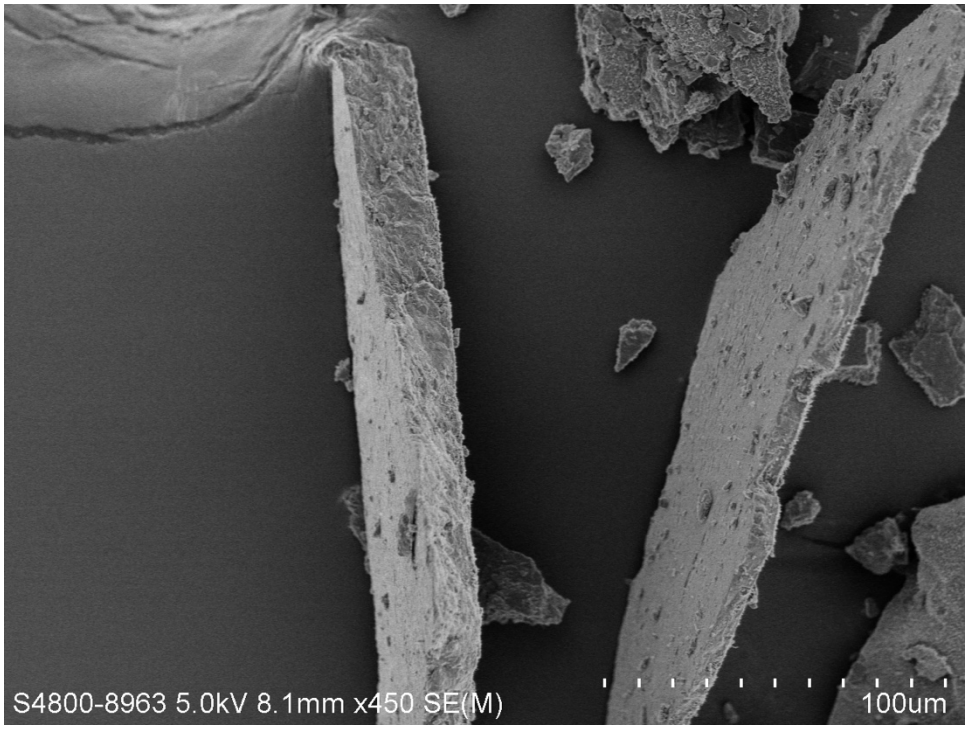


**Figure S2.** PXRD patterns of spray dried ITZ-SUB (SD1-6).

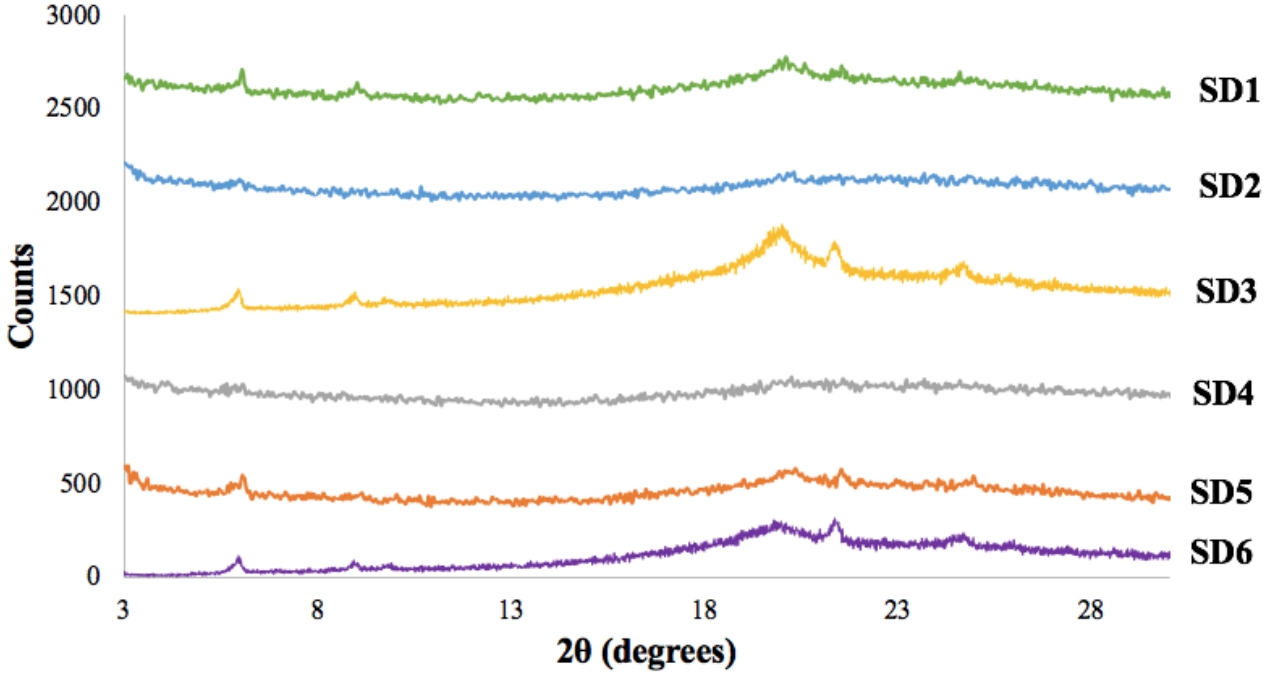

**Figure S3.** DSC profiles of spray dried ITZ-SUB (SD1-6).

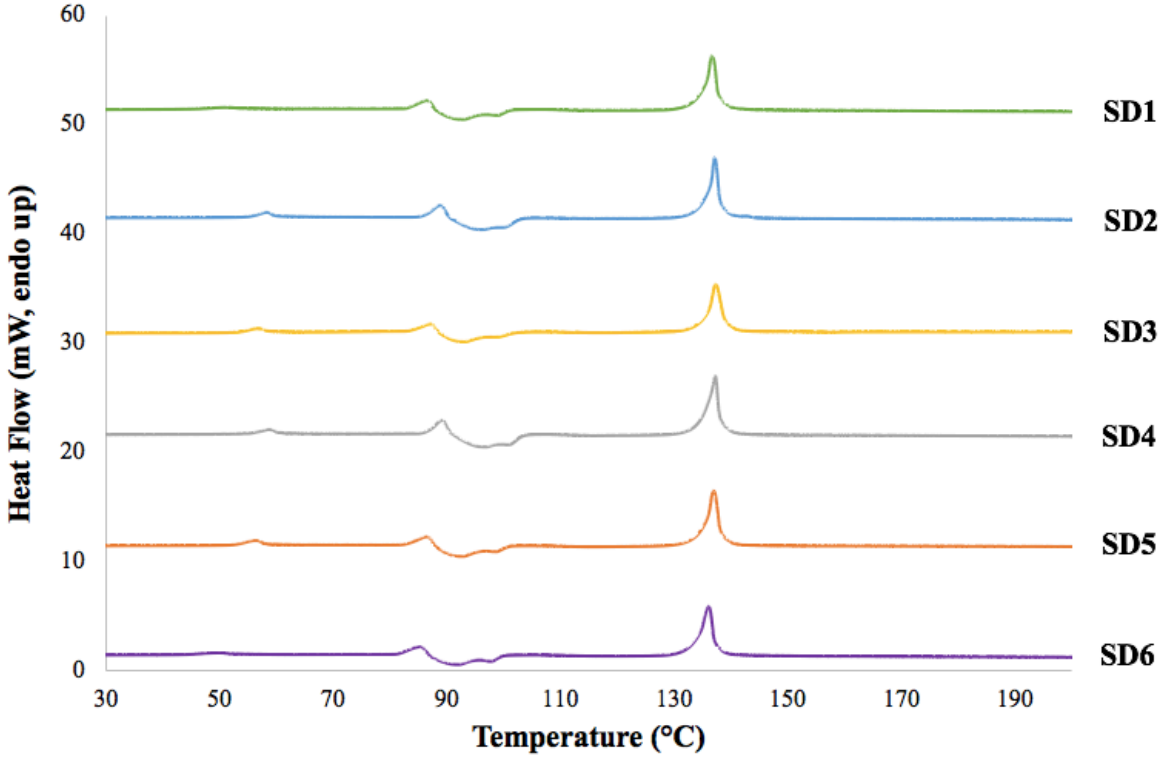


**Figure S4.** FTIR spectra of spray dried ITZ-SUB (SD1-6).

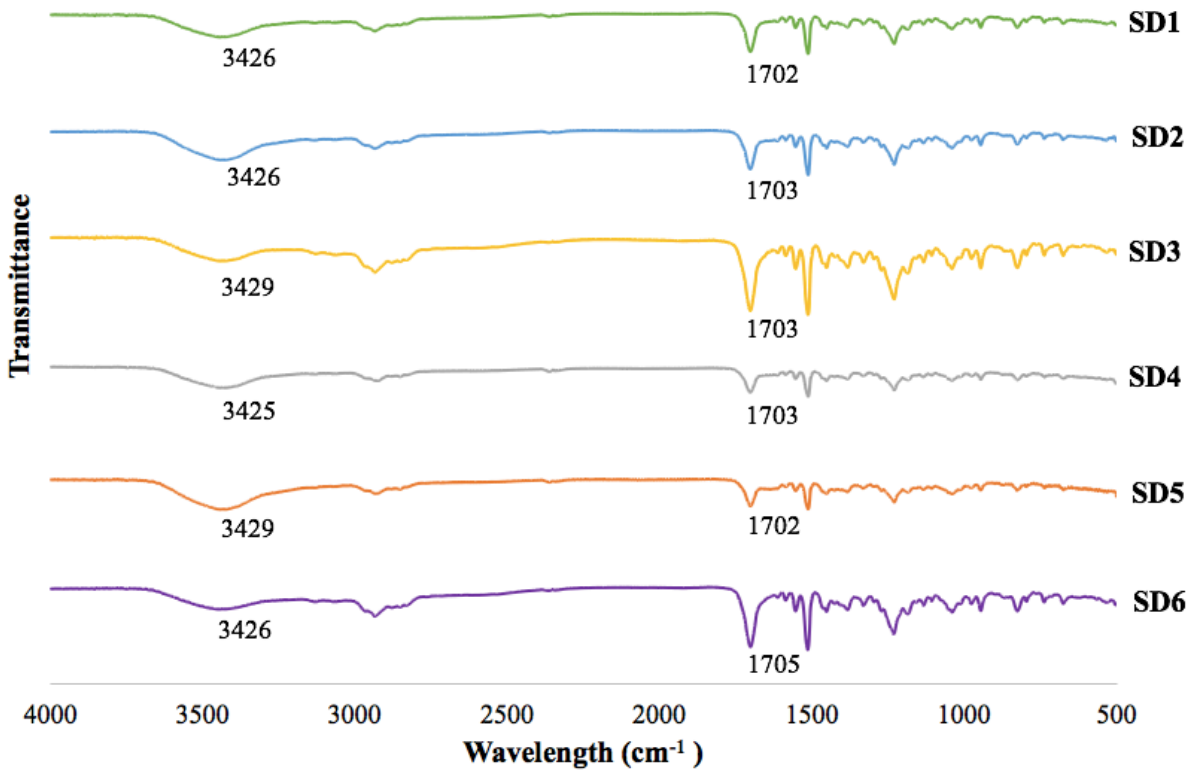

**Figure S5.** SEM images of spray dried ITZ-SUB formulations at 5k× magnification.

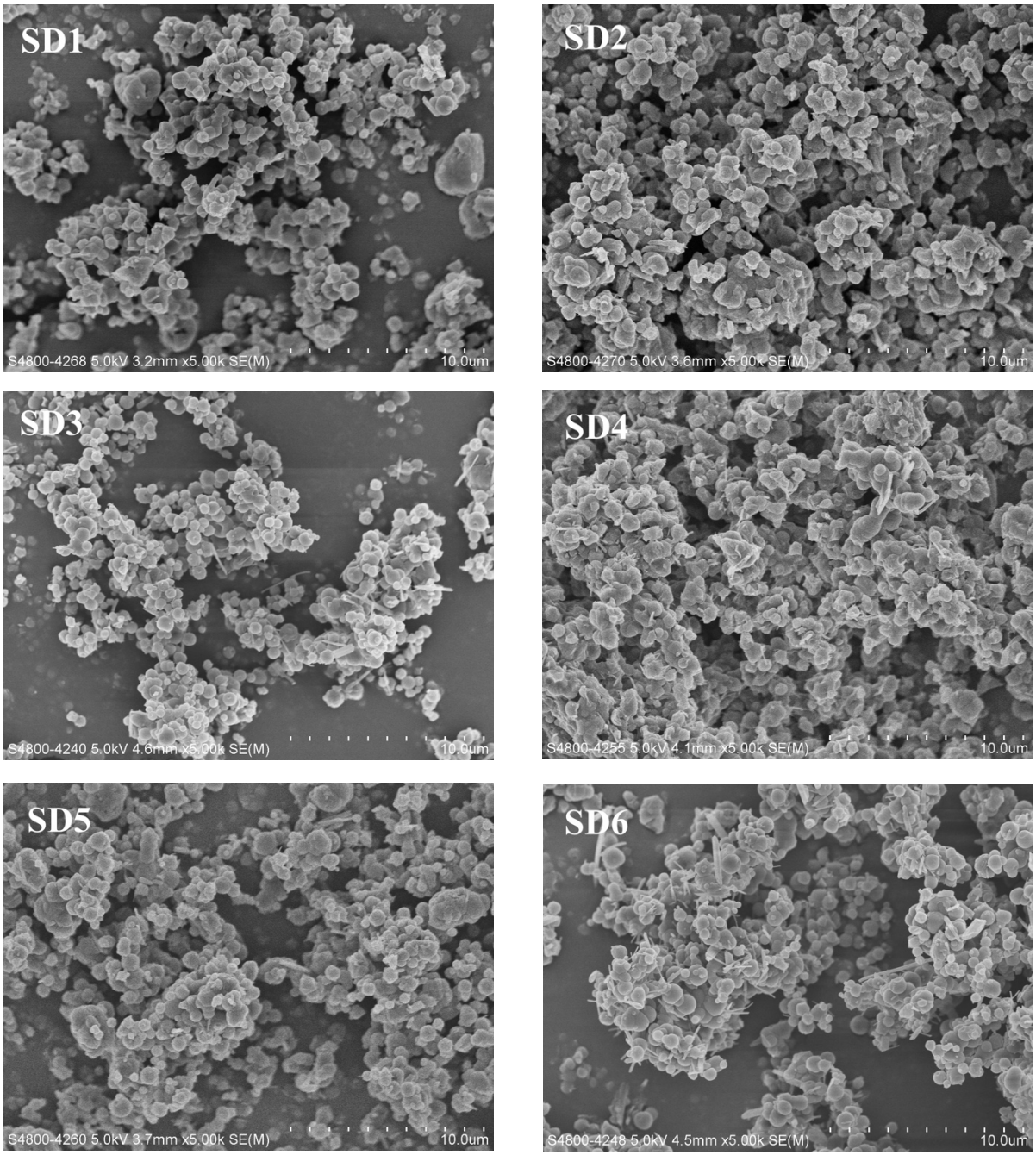

**Figure S6.** NGI dispersion data of spray dried ITZ-SUB.

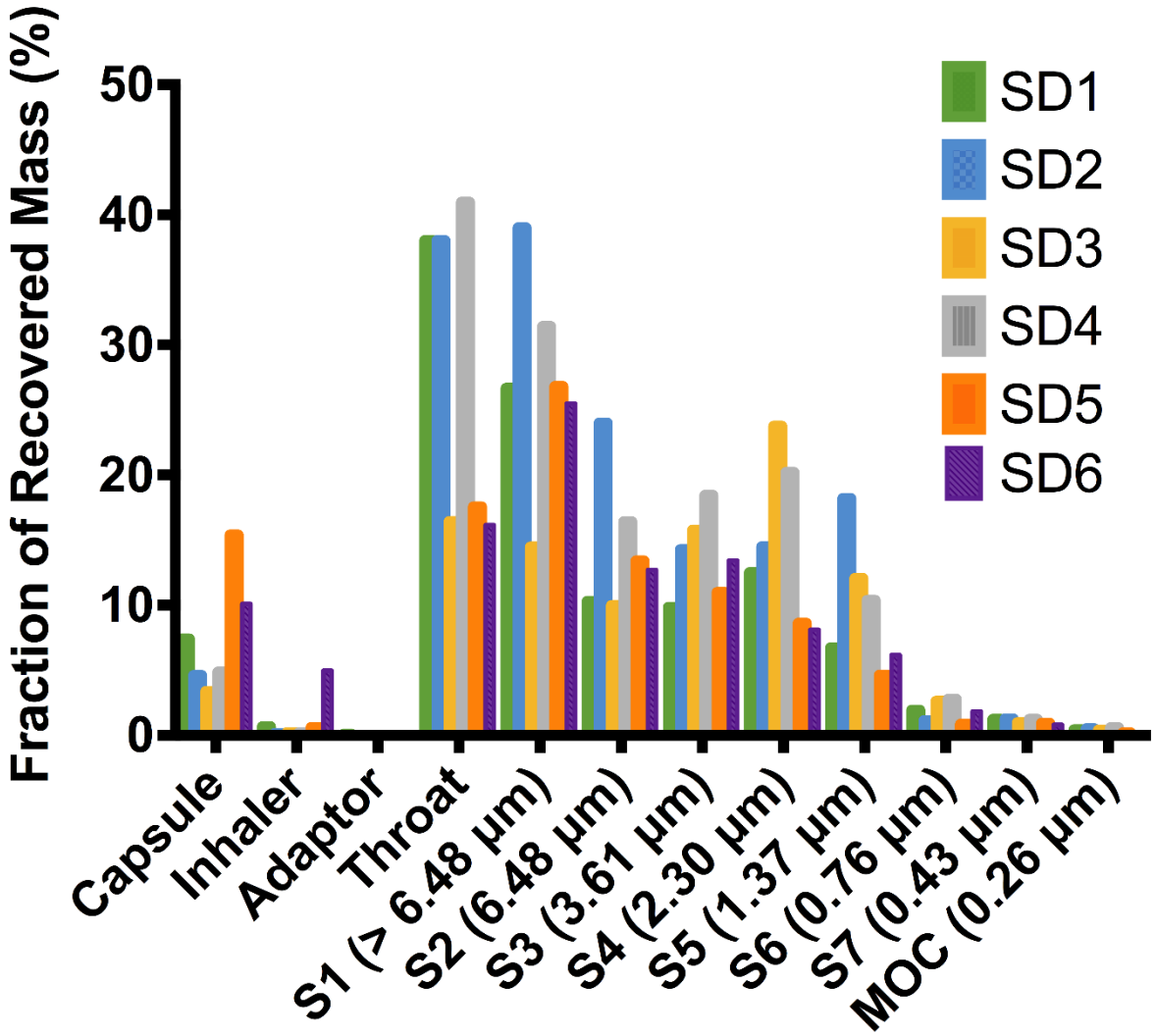

**Figure S7.** SEM images of spray dried ITZ-SUB powders (SD3) deposited on the throat and different stages of the NGI at 5k× magnification.

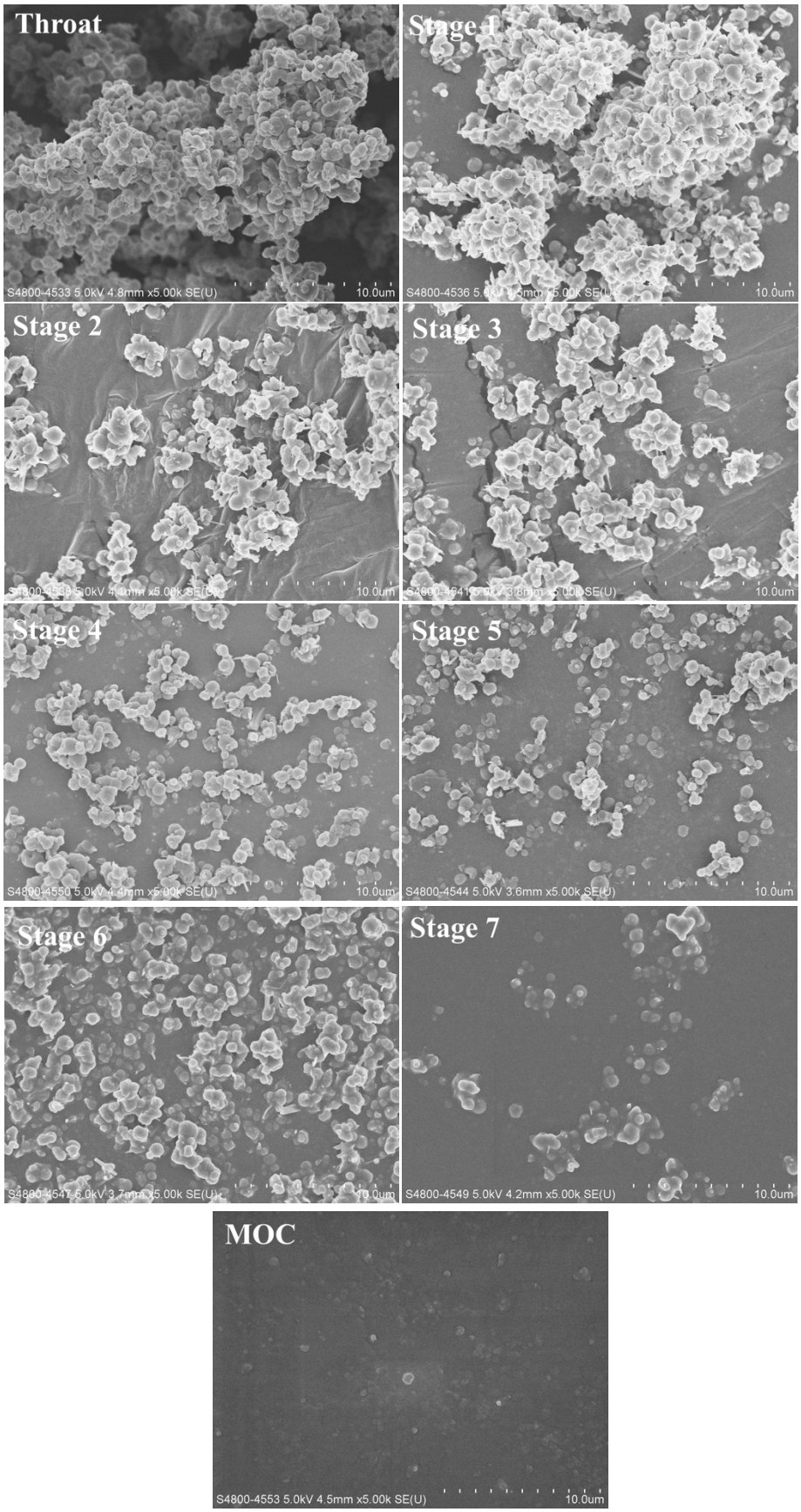

**Figure S8.** SEM images of a) ITZ and b) ITZ-SUB cocrystal.